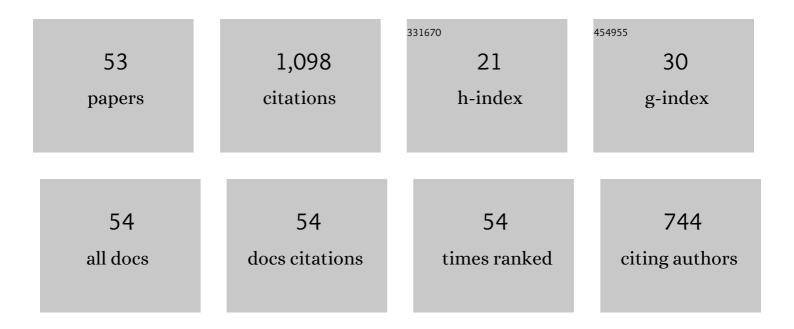
Igor Rahinov

List of Publications by Year in descending order

Source: https://exaly.com/author-pdf/6791806/publications.pdf Version: 2024-02-01



ICOP RAHINOV

#	Article	IF	CITATIONS
1	Early particle formation and evolution in iron-doped flames. Combustion and Flame, 2022, 244, 112251.	5.2	8
2	Experimental and numerical investigation of iron-doped flames: FeO formation and impact on flame temperature. Proceedings of the Combustion Institute, 2021, 38, 1249-1257.	3.9	20
3	Determination of gas-phase absorption cross-sections of FeO in a shock tube using intracavity absorption spectroscopy near 611â€nm. Proceedings of the Combustion Institute, 2021, 38, 1637-1645.	3.9	8
4	NO Binding Energies to and Diffusion Barrier on Pd Obtained with Velocity-Resolved Kinetics. Journal of Physical Chemistry C, 2021, 125, 11773-11781.	3.1	6
5	Absolute concentration imaging using self-calibrating laser-induced fluorescence: application to atomic iron in a nanoparticle flame-synthesis reactor. Applied Physics B: Lasers and Optics, 2021, 127, 1.	2.2	6
6	Insights into the Mechanism of Combustion Synthesis of Iron Oxide Nanoparticles Gained by Laser Diagnostics, Mass Spectrometry, and Numerical Simulations: A Mini-Review. Energy & Fuels, 2021, 35, 137-160.	5.1	21
7	Kinetics of NH ₃ Desorption and Diffusion on Pt: Implications for the Ostwald Process. Journal of the American Chemical Society, 2021, 143, 18305-18316.	13.7	15
8	Particle-in-cell techniques for the study of space charge effects in an electrostatic ion beam trap. Physical Review E, 2021, 104, 065202.	2.1	5
9	Following the microscopic pathway to adsorption through chemisorption and physisorption wells. Science, 2020, 369, 1461-1465.	12.6	42
10	Detailed simulation of iron oxide nanoparticle forming flames: Buoyancy and probe effects. Proceedings of the Combustion Institute, 2019, 37, 1241-1248.	3.9	20
11	Observation of the adsorption and desorption of vibrationally excited molecules on a metal surface. Nature Chemistry, 2018, 10, 592-598.	13.6	70
12	Determination of rate parameters based on NH2 concentration profiles measured in ammonia-doped methane–air flames. Fuel, 2018, 212, 679-683.	6.4	35
13	Concentration measurements by intracavity laser absorption spectroscopy for the case of strongly overlapped spectra. Applied Physics B: Lasers and Optics, 2018, 124, 1.	2.2	2
14	Protein and peptide cross sections and mass spectra in an electrostatic ion beam trap. Journal of Instrumentation, 2017, 12, P05008-P05008.	1.2	5
15	Effect of a localized charge on the stability of Van der Waals clusters. European Physical Journal D, 2016, 70, 1.	1.3	4
16	Vibrational energy transfer near a dissociative adsorption transition state: State-to-state study of HCl collisions at Au(111). Journal of Chemical Physics, 2016, 145, 054709.	3.0	29
17	Activated Dissociation of HCl on Au(111). Journal of Physical Chemistry Letters, 2016, 7, 1346-1350.	4.6	29
18	Experimental and modelling study of 1CH2 in premixed very rich methane flames. Combustion and Flame, 2016, 171, 198-210.	5.2	37

Igor Rahinov

#	Article	IF	CITATIONS
19	Pulsed Flame for Syngas Production via Partial Methane Oxidation. Flow, Turbulence and Combustion, 2016, 96, 363-375.	2.6	0
20	New Perspectives in Monitoring the Flame Synthesis of Iron Oxide Nanoparticles: Addressing Solid and Gas-Phase Diagnostics Challenges. Materials Research Society Symposia Proceedings, 2015, 1747, 7.	0.1	1
21	Intracavity Laser Absorption Spectroscopy Study of HCO Radicals during Methane to Hydrogen Conversion in Very Rich Flames. Energy & Fuels, 2015, 29, 6146-6154.	5.1	5
22	Initial reaction steps during flame synthesis of iron-oxide nanoparticles. CrystEngComm, 2015, 17, 6930-6939.	2.6	41
23	A fiber laser intracavity absorption spectroscopy (FLICAS) sensor for simultaneous measurement of CO and CO2 concentrations and temperature. Sensors and Actuators B: Chemical, 2015, 210, 431-438.	7.8	22
24	Fiber Laser Intracavity Spectroscopy of hot water for temperature and concentration measurements. Applied Physics B: Lasers and Optics, 2015, 121, 345-351.	2.2	4
25	On the mechanism of nanoparticle formation in a flame doped by iron pentacarbonyl. Physical Chemistry Chemical Physics, 2015, 17, 680-685.	2.8	20
26	A method for nanoparticle characterization by laser induced detuning of quartz crystal microbalance (LID-QCM). Sensors and Actuators B: Chemical, 2014, 202, 861-865.	7.8	4
27	The importance of accurate adiabatic interaction potentials for the correct description of electronically nonadiabatic vibrational energy transfer: A combined experimental and theoretical study of $NO(\langle i \rangle v \langle i \rangle = 3)$ collisions with a Au(111) surface. Journal of Chemical Physics, 2014, 140, 044701.	3.0	39
28	Incidence energy dependent state-to-state time-of-flight measurements of NO($v = 3$) collisions with Au(111): the fate of incidence vibrational and translational energy. Physical Chemistry Chemical Physics, 2014, 16, 7602.	2.8	16
29	Absorption electronic spectrum of gaseous FeO: in situ detection with intracavity laser absorption spectroscopy in a nanoparticle-generating flame reactor. Applied Physics B: Lasers and Optics, 2014, 117, 317-323.	2.2	13
30	Combined particle mass spectrometer – Quartz crystal microbalance apparatus for in situ nanoparticle monitoring during flame assisted synthesis. Combustion and Flame, 2013, 160, 2131-2140.	5.2	17
31	Experimental and Theoretical Study of Multi-Quantum Vibrational Excitation: NO(<i>v</i> = 0→1,2,3) in Collisions with Au(111). Journal of Physical Chemistry A, 2013, 117, 7091-7101.	2.5	22
32	State-to-State Time-of-Flight Measurements of NO Scattering from Au(111): Direct Observation of Translation-to-Vibration Coupling in Electronically Nonadiabatic Energy Transfer. Journal of Physical Chemistry A, 2013, 117, 8750-8760.	2.5	34
33	On the determination of absolute vibrational excitation probabilities in molecule-surface scattering: Case study of NO on Au(111). Journal of Chemical Physics, 2012, 137, 064705.	3.0	20
34	Lifetime measurements in an electrostatic ion beam trap using image charge monitoring. Review of Scientific Instruments, 2012, 83, 033302.	1.3	16
35	Vibrational excitation and relaxation of NO molecules scattered from a Au (111) surface. , 2012, , .		1
36	Blackbody-induced radiative dissociation of cationic SF <mml:math xmlns:mml="http://www.w3.org/1998/Math/MathML" display="inline"><mml:msub><mml:mrow /><mml:mn>6</mml:mn></mml:mrow </mml:msub>clusters. Physical Review A, 2012, 86, .</mml:math 	2.5	15

Igor Rahinov

#	Article	IF	CITATIONS
37	Multiquantum Vibrational Excitation of NO Scattered from Au(111): Quantitative Comparison of Benchmark Data to Abâ€Initio Theories of Nonadiabatic Molecule–Surface Interactions. Angewandte Chemie - International Edition, 2012, 51, 4954-4958.	13.8	39
38	On the temperature dependence of electronically non-adiabatic vibrational energy transfer in molecule–surface collisions. Physical Chemistry Chemical Physics, 2011, 13, 8153-8162.	2.8	20
39	Quantifying the breakdown of the Born–Oppenheimer approximation in surface chemistry. Physical Chemistry Chemical Physics, 2011, 13, 12680.	2.8	44
40	In situmeasurement of the mass concentration of flame-synthesized nanoparticles using quartz-crystal microbalance. Measurement Science and Technology, 2011, 22, 115102.	2.6	7
41	Vibrational overtone excitation in electron mediated energy transfer at metal surfaces. Chemical Science, 2010, 1, 55.	7.4	27
42	Efficient translational excitation of a solid metal surface: State-to-state translational energy distributions of vibrational ground state HCl scattering from Au(111). Journal of Vacuum Science and Technology A: Vacuum, Surfaces and Films, 2009, 27, 907-912.	2.1	27
43	Efficient vibrational and translational excitations of a solid metal surface: State-to-state time-of-flight measurements of HCl(v=2,J=1) scattering from Au(111). Journal of Chemical Physics, 2008, 129, 214708.	3.0	51
44	Intracavity Laser Absorption Spectroscopy for flame diagnostics. Israel Journal of Chemistry, 2007, 47, 131-140.	2.3	11
45	Absorption spectroscopy diagnostics of amidogen in ammonia-doped methane/air flames. Combustion and Flame, 2006, 145, 105-116.	5.2	38
46	Fiber laser intracavity absorption spectroscopy of ammonia and hydrogen cyanide in low pressure hydrocarbon flames. Chemical Physics Letters, 2006, 423, 147-151.	2.6	25
47	Molecular oxygen detection in low pressure flames using cavity ring-down spectroscopy. Applied Physics B: Lasers and Optics, 2006, 82, 659-663.	2.2	13
48	Intracavity laser absorption spectroscopy and cavity ring-down spectroscopy in low-pressure flames. Applied Physics B: Lasers and Optics, 2005, 81, 143-149.	2.2	23
49	Intracavity laser absorption spectroscopy of NH2 in methane/air flames doped with N2O, NO, and NH3. Proceedings of the Combustion Institute, 2005, 30, 1575-1582.	3.9	11
50	NH2 radical formation by ammonia pyrolysis in a temperature range of 800?1000�K. Applied Physics B: Lasers and Optics, 2003, 77, 541-546.	2.2	39
51	Intracavity laser absorption spectroscopy measurements of CN using red system A–X. Simultaneous observation of CN, NH2, HNO and in low pressure hydrocarbon flames doped with nitrogen oxides. Chemical Physics Letters, 2002, 352, 169-175.	2.6	19
52	Laser absorption spectroscopy diagnostics of nitrogen-containing radicals in low-pressure hydrocarbon flames doped with nitrogen oxides. Faraday Discussions, 2001, 119, 321-335.	3.2	17
53	Absorption spectroscopy measurements of NH and NH2 absolute concentrations in methane/air flames doped with N2O. Proceedings of the Combustion Institute, 2000, 28, 1741-1748.	3.9	19